

# Two-body continuum states in non-integer geometry

E.R. Christensen<sup>2</sup>, E. Garrido<sup>1</sup>, A.S. Jensen<sup>2</sup>

<sup>1</sup>*Instituto de Estructura de la Materia, IEM-CSIC, Serrano 123, E-28006 Madrid, Spain and*

<sup>2</sup>*Department of Physics and Astronomy, Aarhus University, DK-8000 Aarhus C, Denmark*

(Dated: March 3, 2022)

Wave functions, phase shifts and corresponding elastic cross sections are investigated for two short-range interacting particles in a deformed external oscillator field. For this we use the equivalent  $d$ -method employing a non-integer dimension  $d$ . Using a square-well potential, we derive analytic expressions for scattering lengths and phase shifts. In particular, we consider the dimension,  $d_E$ , for infinite scattering length, where the Efimov effect occurs by addition of a third particle. We give explicitly the equivalent continuum wave functions in  $d$  and ordinary three dimensional (3D) space, and show that the phase shifts are the same in both methods. Consequently the  $d$ -method can be used to obtain low-energy two-body elastic cross sections in an external field.

## I. INTRODUCTION

The experimental possibilities with cold atomic gases allow both huge two-body interaction variation as well as an overall confining deformed external field [1–4]. Few-body physics quickly becomes complicated or even impossible as the number of particles increase, and other techniques have to be employed, see for example [5]. One purpose of studying these cold systems is the experimental availability, where laboratory simulation and manipulation are possible. These systems may themselves be of practical use, but also able to teach us how to control and create similar properties in systems, which so far are outside of experimental reach. Comparing universal behavior of systems from different subfields of physics, perhaps also chemistry and mathematics, is then a tool to exchange knowledge between science subfields [6–14].

The advantage of few-body physics is that all relevant degrees-of-freedom can be accurately treated. Increasing the number of particles from two to three is known to increase substantially the complications, like the appearance of new possible structures, but also the interest. The complications are accentuated by use of overall external fields, where the description requires more than relative degrees-of-freedom. It is then worth cashing in on a reduction of degrees-of-freedom, which is very useful, by means of the use of an effective dimension that changes continuously [9, 15–18].

We shall in this report concentrate on the  $d$ -method, introduced in Ref. [9], and subsequently developed and applied for two and three particles [19–22, 24]. The theoretical formulation assumes non-integer dimensions,  $d$ , only relative degrees of freedom, but with a  $d$ -dependent angular momentum barrier, and spherical calculations without angular dependence corresponding to zero angular momentum for  $d = 3$ . The equivalence to the description with an external deformed oscillator potential is available, such that the  $d$ -method results can be translated to ordinary three-dimensional calculations, and in this way open for experimental comparison [24].

Interesting features revealed and highlighted by this method can be understood from the continuous change of dimension from 3 to 2. The properties of quantum

solutions for simple two-body systems differ enormously between these two dimensions. For  $d = 3$ , even for relative  $s$ -waves, a finite attraction is necessary to bind, whereas for  $d = 2$  and relative  $s$ -waves, an infinitely small attraction produces a bound state [13, 25–28]. For three particles the differences are much larger, as emphasized by the existing Efimov effect for  $d = 3$ , defined by no bound two-body subsystems, but infinitely many bound three-body systems. In contrast, only a finite number of bound states exist for  $d = 2$ . Thus varying  $d$  between 3 and 2 necessarily implies that some states must change behavior from bound to continuum states or vice versa. One especially spectacular phenomenon is that the Efimov effect can be induced between dimensions 3 and 2, while absent in both ends of the interval [24].

The  $d$ -variation amounts to varying an external field, which is a familiar procedure. This is exemplified from the Feshbach tuning of a magnetic field allowing huge changes of the effective two-body interaction [29, 30]. This is the same principle as for variation of an external electric field as first suggested in Ref. [31]. The present use of the  $d$ -method can then be viewed as a theoretical application of an external field without the necessary additional degrees-of-freedom. However, these fields are unavoidable when comparing with practical experiments.

Continuum or scattering calculations are usually more difficult than bound state investigations [32]. It is therefore tempting to extend the  $d$ -method to the continuum, and first to learn from the simplest system, that is, a two-body system. The task is then to perform calculations with the  $d$ -method, and subsequently translate or interpret the results to three dimensions with an external field. We shall study two particles interacting through simple short-range potentials. The main properties can then be revealed by square-well potentials, from which we can derive analytic solutions with characteristic universal behavior. These square-well results may be compared to numerically found solutions for more realistic Gaussian potentials.

The purpose of the present report is therefore to study continuum properties of two-body systems with the  $d$ -method, and interpret as if obtained in an external field with the possible experimental comparison. Special at-

tention will be paid to the dimension,  $d = d_E$ , for which the two-body binding energy is equal to zero. This dimension is particularly interesting, since for  $d = d_E$  the Efimov conditions are fulfilled if a third particle is added.

After the introduction in Section I, we derive in Section II several analytical expressions of interest assuming a square-well interaction. In the different subsections we provide the energy of bound states as a function of  $d$  and of the strength of the potential, the critical dimension  $d_E$  as a function of the strength of the potential, and the phase shifts also as a function of  $d$  and of the strength of the potential. Finally, we also discuss in this section how these phase shifts have to be treated in order to construct the cross sections. The results and illustrations are provided in Section III, where together with the direct applications of the expressions derived in Section II, we focus on the universality of the results, investigating how the values of  $d_E$  and the phase shifts can be shown to present a universal behavior, independent of the details of the potential. We finish with Section IV, which contains the summary and conclusions. Pertinent properties of the Bessel functions are collected in an appendix.

## II. TWO-BODY SCATTERING

We consider the two-body problem in  $d$  dimensions, where  $2 \leq d \leq 3$ , and where the two-body interaction is assumed to be of short range. Using a schematic short-range square-well potential, we shall derive expressions for bound- and continuum-state energies, threshold conditions, phase shifts, scattering lengths, and cross sections, all as a function of  $d$ . In the end, these results can be interpreted as obtained by an external deformed field and full three-dimensional space.

The derived analytic properties, properly expressed, exhibit the highly desired universal behavior. This universality means potential independence at distances larger than the radius of the short-range interaction. In other words, gross properties are sufficient to describe the results for relatively small energies. Numerical calculations using a Gaussian potential will be used as an illustration.

### A. Theoretical formulation

For two-body systems and dimension  $d$ , the reduced,  $R(r)$ , and the total,  $\psi(r)$ , radial relative wave functions are related by  $R(r) = r^{(d-1)/2}\psi(r)$ , where  $r$  is the relative distance coordinate. The reduced wave function,  $R(r)$ , is obtained as a solution, with the proper boundary conditions, of the  $d$ -dimensional radial Schrödinger equation for the relative motion [9]:

$$\left[ -\frac{\hbar^2}{2\mu} \left( \frac{\partial^2}{\partial r^2} - \frac{\ell^*(\ell^* + 1)}{r^2} \right) + V(r) - E \right] R(r) = 0, \quad (1)$$

where  $V(r)$  is the spherical potential and  $\mu$  the reduced mass. For two-body systems the effective angular momentum  $\ell^*$  takes the form

$$\ell^* = \ell_{2b} + \frac{d-3}{2}, \quad (2)$$

where  $\ell_{2b}$  is the relative orbital angular momentum between the two particles.

All along the squeezing process, the momentum  $\ell_{2b}$  is a good quantum number, which for  $d = 3$  becomes the usual orbital angular momentum. Also, when confining from three to two dimensions by means of an external squeezing potential, it is known that the angular momentum projection quantum number,  $m$ , is conserved [21], and, furthermore,  $m$  is the angular momentum in the two-dimension limit [9]. Therefore, for  $d = 2$  we have  $m = \ell_{2b}$ , which, due to the conservation of  $m$ , implies that the same equality holds for the initial non-squeezed 3D-state as well.

Let us assume  $V(r)$  is a spherical square-well potential, that is

$$V(r) = \begin{cases} -V_0, & r < r_0 \\ 0 & r > r_0 \end{cases}, \quad (3)$$

where  $V_0 (> 0)$  is the depth and  $r_0$  the radius.

After introducing the dimensionless variable  $x = r/r_0$ , the equation *inside* the box,  $r < r_0$  ( $x < 1$ ), then reads

$$\left[ -\frac{\partial^2}{\partial x^2} + \frac{\ell^*(\ell^* + 1)}{x^2} - k^2 \right] R_{in}(x) = 0, \quad (4)$$

and similarly outside the box,  $r > r_0$  ( $x > 1$ ),

$$\left[ -\frac{\partial^2}{\partial x^2} + \frac{\ell^*(\ell^* + 1)}{x^2} - \kappa^2 \right] R_{out}(x) = 0, \quad (5)$$

where the wave numbers are given by

$$k = \sqrt{\frac{2\mu r_0^2(E + V_0)}{\hbar^2}}, \quad \kappa = \sqrt{\frac{2\mu r_0^2 E}{\hbar^2}}. \quad (6)$$

Note that  $\kappa$  is imaginary for bound states, but real and positive for continuum states.

The solution inside the box,  $R_{in}$ , is simply given by

$$R_{in}(x) = A_k x j_{\ell^*}(kx), \quad (7)$$

where  $j_{\ell^*}$  is the spherical Bessel function of first kind and  $A_k$  is a normalization constant. The other Bessel function,  $\eta_{\ell^*}$ , also a solution to Eq.(4), diverges at  $x = 0$  and is therefore removed from Eq.(7), since the physical solution must satisfy that  $R_{in}(x) \rightarrow 0$  for  $x \rightarrow 0$ . Note that  $\ell^*$  is in general non-integer, and even negative for  $s$ -waves ( $\ell_{2b} = 0$ ) when  $d < 3$  ( $\ell^* = (d-3)/2$ ).

## B. Bound states

For a bound state ( $E < 0$  and  $\kappa = i|\kappa|$ ), the solution outside the box,  $R_{out}(x)$ , takes the form

$$R_{out}(x) = B_\kappa x h_{\ell^*}^{(+)}(\kappa x), \quad (8)$$

where  $h_{\ell^*}^{(+)}$  is the spherical Hankel function of first kind and  $B_\kappa$  is a normalization constant. The other Hankel function solution to Eq.(5),  $h_{\ell^*}^{(-)}(\kappa x)$ , is removed, since the bound state solution must fall off exponentially at large distance.

Matching the logarithmic derivatives of Eqs.(7) and (8) at the box radius,  $x = 1$ , we obtain the eigenvalue equation for bound states. The normalization factors disappear and we find, by use of the two identities Eqs.(A2) and (A3), that

$$1 + \ell^* - k \frac{j_{\ell^*+1}(k)}{j_{\ell^*}(k)} = 1 + \ell^* - \kappa \frac{h_{\ell^*+1}^{(+)}(\kappa)}{h_{\ell^*}^{(+)}(\kappa)}, \quad (9)$$

where the left and right hand sides in Eq.(9) are the logarithmic derivatives of the solutions inside and outside the box, respectively.

Eq.(9) is an equation relating the square-well parameter,  $S_0$ , and  $\kappa$  in Eq.(6) through

$$S_0^2 \equiv \frac{2\mu r_0^2 V_0}{\hbar^2}, \quad k^2 = S_0^2 + \kappa^2. \quad (10)$$

In other words, the bound state energy,  $E$ , in units of  $\hbar^2/(\mu r_0^2)$ , is a unique function of the square-well parameter,  $S_0$ . The oscillatory behavior of the Bessel functions provides more and more discrete energy solutions with increasing  $S_0$ . All this is in complete analogy to the usual square-well relative two-body problem, but now depending on  $\ell^*$ , and therefore on  $d$ .

## C. Efimov condition

Let us consider now a moderate square-well parameter,  $S_0$ , which is too small to support any bound state for  $d = 3$ . However, if the system is bound in two dimensions, we then know that, when decreasing  $d$  from 3 to 2, a bound state of zero energy must appear at some value,  $d = d_E$ . This always happens for  $s$ -waves ( $\ell_{2b} = 0$ ), since for  $d = 2$  a bound state is always present, even for an infinitesimal attraction. We label this dimension,  $d_E$ , because if an additional particle is added, the resulting three-body system would exhibit Efimov properties, if at least two of the two-body subsystems, in a relative  $s$ -wave, are bound by precisely zero energy. In particular, if dealing with identical particles, this critical value,  $d_E$ , is therefore the non-integer dimension where the Efimov effect occurs on the path towards two dimensions [22].

To find an expression for  $d_E$ , we take the limit  $E \rightarrow 0^-$  in the eigenvalue equation, Eq.(9). This means that  $\kappa \rightarrow$

0, and  $k \rightarrow \sqrt{2\mu r_0^2 V_0/\hbar^2} = S_0$ . Using the low-energy expansion of the Bessel-functions, Eq.(A4), we easily get:

$$\kappa \frac{h_{\ell^*+1}^{(+)}(\kappa)}{h_{\ell^*}^{(+)}(\kappa)} \rightarrow 2\ell^* + 1. \quad (11)$$

The eigenvalue equation, Eq.(9), reduces then to

$$S_0 \frac{j_{\ell^*+1}(S_0)}{j_{\ell^*}(S_0)} = 2\ell^* + 1 = 2\ell_{2b} + d_E - 2, \quad (12)$$

which is the condition for a zero-energy solution, and therefore gives  $d = d_E$  as a function of the square-well parameter,  $S_0$ . We emphasize that the index,  $\ell^*$ , on the Bessel function depends on  $d$  as expressed in Eq.(2).

It is important to note here that the philosophy of studying scattering properties through an extension of the angular momentum to non-integer values,  $\ell^*$ , is akin to the concept of Regge poles, where the angular momentum is generalized to a continuum, and even complex, variable, and the analytical behavior of the  $S$ -matrix is subsequently studied. In fact, Eq.(12) can be simplified into:

$$J_{\ell^*-\frac{1}{2}}(S_0) = 0, \quad (13)$$

which, as shown in [36], determines the zero-energy position of the Regge poles for the square-well potential. Therefore, the critical dimension,  $d_E$ , for a given  $S_0$  value corresponds to the zero-energy Regge pole of the potential.

## D. Scattering length

The zero-energy condition is closely related to the scattering length, which also must depend on the dimension  $d$ . We derive an expression by first noting that the zero-energy reduced radial wave function must by definition have the form [9]

$$R_{out}(x) \propto x^{\ell^*+1} - \frac{(a_d^{(\ell^*)}/r_0)^{2\ell^*+1}}{x^{\ell^*}}, \quad (14)$$

expressed in terms of the scattering length,  $a_d^{(\ell^*)}$  divided by the length unit,  $r_0$ . We used that the reduced,  $R$ , and total,  $\psi$ , radial wave functions are related by  $R(x) = x^{(d-1)/2}\psi(x)$ .

Matching the logarithmic derivatives of Eqs.(7) and (14) at  $x = 1$ , we get

$$1 + \ell^* - S_0 \frac{j_{\ell^*+1}(S_0)}{j_{\ell^*}(S_0)} = \frac{1 + \ell^* + \ell^* \left(\frac{a_d^{(\ell^*)}}{r_0}\right)^{2\ell^*+1}}{1 - \left(\frac{a_d^{(\ell^*)}}{r_0}\right)^{2\ell^*+1}}, \quad (15)$$

which immediately leads to

$$\frac{a_d^{(\ell^*)}}{r_0} = \left(1 - \frac{(2\ell^* + 1)j_{\ell^*}(S_0)}{S_0 j_{\ell^*+1}(S_0)}\right)^{-1/(2\ell^*+1)}. \quad (16)$$

The scattering length depends on  $S_0$  and  $\ell^*$ , or  $S_0$ ,  $d$  and  $\ell_{2b}$ , in units of the square-well radius.

We see from Eq.(12) that this scattering length,  $a_d^{(\ell^*)}$ , is infinitely large exactly when  $d = d_E$ . Another consistency check is for  $d = 3$  and  $\ell_{2b} = 0$  ( $\ell^* = 0$ ), where Eq.(16) reduces to the well-known expression:

$$\frac{a_{d=3}^{(\ell^*=0)}}{r_0} = 1 - \frac{\tan(S_0)}{S_0}. \quad (17)$$

### E. Phase-shifts

Let us consider now the case of continuum states ( $E > 0$ ). The large-distance solution in Eq.(8) should be replaced by

$$R_{out}(x) = x(\cos \delta_{\ell^*} j_{\ell^*}(\kappa x) - \sin \delta_{\ell^*} \eta_{\ell^*}(\kappa x)), \quad (18)$$

where  $\eta_{\ell^*}$  is the irregular Bessel function, and  $\delta_{\ell^*}$  is the phase-shift corresponding to this continuum state of generalized angular momentum  $\ell^*$  and energy  $E$ .

The solution of  $\delta_{\ell^*}$  as function of  $E$  and  $\ell^*$  is found by matching the logarithmic derivatives of Eqs.(7) and (18), that is

$$\frac{k j'_{\ell^*}(k)}{\kappa j_{\ell^*}(k)} = \frac{\cot \delta_{\ell^*} j'_{\ell^*}(\kappa) - \eta'_{\ell^*}(\kappa)}{\cot \delta_{\ell^*} j_{\ell^*}(\kappa) - \eta_{\ell^*}(\kappa)}, \quad (19)$$

where the prime denotes derivative with respect to the full argument of the function. The phase-shift can then be calculated from Eq.(19) to give

$$\cot \delta_{\ell^*} = \frac{\eta_{\ell^*}(\kappa) \kappa \frac{j_{\ell^*+1}(\kappa)}{\eta_{\ell^*}(\kappa)} - k \frac{j_{\ell^*+1}(k)}{j_{\ell^*}(k)}}{j_{\ell^*}(\kappa) \kappa \frac{j_{\ell^*+1}(\kappa)}{j_{\ell^*}(\kappa)} - k \frac{j_{\ell^*+1}(k)}{j_{\ell^*}(k)}}, \quad (20)$$

where we used the derivative expressions for both  $j_{\ell^*}$  and  $\eta_{\ell^*}$  from Eqs.(A2) and (A3).

The low-energy limits,  $\kappa \rightarrow 0$ ,  $k \rightarrow S_0$ , are then to leading order obtained from Eq.(A4),

$$\cot \delta_{\ell^*} \rightarrow \frac{-1}{(2\ell^* + 1)\kappa^{2\ell^*+1}} \quad (21)$$

$$\times \left( \frac{\Gamma(2\ell^* + 2)}{2^{\ell^*} \Gamma(\ell^* + 1)} \right)^2 \times \left( 1 - \frac{(2\ell^* + 1)j_{\ell^*}(S_0)}{S_0 j_{\ell^*+1}(S_0)} \right),$$

where  $\Gamma$  is the usual Gamma function.

Note that for  $d = d_E$ , making use of Eq.(12) in the last bracket of Eq.(21), we get that  $\cot \delta_{\ell^*} = 0$ , or, in other words,  $\delta_{\ell^*} = \pi/2$ .

Assuming that the low-energy limit of the phase-shift is proportional to  $\kappa^{2\ell^*+1}$ , we can express this limit in terms of the scattering length in Eq.(16), that is

$$\delta_{\ell^*} \rightarrow -(2\ell^* + 1) \frac{2^{2\ell^*} \Gamma^2(\ell^* + 1)}{\Gamma^2(2\ell^* + 2)} \left( 2\mu E [a_d^{(\ell^*)}]^2 / \hbar^2 \right)^{\frac{2\ell^*+1}{2}} \quad (22)$$

### F. Cross sections

As mentioned several times, the  $d$ -method has been introduced as a tool that simplifies the description of systems squeezed due to the presence of an external field. It is obvious that any observable will be measured in the squeezed 3D space, and therefore, in order to compare the calculations with whatever available experimental data, it is necessary to translate the observable from the  $d$ -dimensional space into the 3D space.

This is in particular necessary when computing cross sections. It is not obvious that the phase shifts derived in the previous subsection can be directly employed to get the cross sections simply by using them in the usual 3D cross section expressions in terms of the phase shifts.

To understand how to proceed, we first interpret the  $d$ -dimensional wave function as described in [20], that is, as a wave function in the ordinary 3D space where the relative coordinate in the  $d$ -space,  $\mathbf{r}$ , is now understood as a 3D vector, denoted as  $\tilde{\mathbf{r}}$ , but where the third coordinate (the  $z$ -axis is chosen along the squeezing direction) is squeezed by means of a scale parameter  $s$ . In other words, the  $d$ -coordinate,  $\mathbf{r}$ , is then understood as a 3D-coordinate as:

$$\mathbf{r} \rightarrow \tilde{\mathbf{r}} = (x, y, \tilde{z}) = (x, y, \frac{z}{s}), \quad (23)$$

where  $x$ ,  $y$ , and  $z$  are the usual Cartesian coordinates in 3D of the actual relative coordinate,  $r$ , in the 3D-squeezed space. In this way:

$$\tilde{r}^2 = x^2 + y^2 + \frac{z^2}{s^2} = r_{\perp}^2 + \frac{z^2}{s^2} = r^2 \left( \sin^2 \theta + \frac{\cos^2 \theta}{s^2} \right), \quad (24)$$

where  $\theta$  is the usual polar angle.

In the same way, the direction of the 3D-coordinate,  $\tilde{\mathbf{r}}$ , is given by the polar and azimuthal angles  $\tilde{\theta} = \arctan(r_{\perp}/\tilde{z})$  and  $\tilde{\varphi} = \arctan(y/x)$ . They can be easily related to the polar and azimuthal angles of the actual relative coordinate,  $\theta = \arctan(r_{\perp}/z)$  and  $\varphi = \arctan(y/x)$ , leading to:

$$\tan \theta = \frac{1}{s} \tan \tilde{\theta}, \quad \varphi = \tilde{\varphi}, \quad (25)$$

which reflects the fact that the squeezing is taken along the  $z$ -axis, and in the case of large squeezing (very small  $s$ ) only values of  $\theta$  very close to  $\theta = \pi/2$  are allowed, as it corresponds to a system moving in the  $xy$ -plane.

To determine the value of the scale parameter  $s$  we use the approximate expression derived in [22]:

$$\frac{1}{s^2} = \left[ 1 + \left( \frac{(3-d)(d-1)}{2(d-2)} \right)^2 \right]^{1/2}, \quad (26)$$

which is based on the assumption of harmonic oscillator particle-particle interactions. For identical particles, only the harmonic frequency of the interaction enters and it

can be adjusted to give the same  $d = 2$  binding energy as the general short-range interaction. Numerical tests show that this is a good approximation [22].

However, for continuum states this interpretation of the radial coordinates is still not enough. Even for very small values of the scale parameter  $s$  (which imply a large squeezing along the  $z$ -direction) the asymptotic wave function (18) is still oscillating, and not vanishing, for sufficiently large values of  $z$ . Therefore, it is necessary to introduce an additional factor imposing the confinement along the squeezing direction. In particular, assuming a harmonic oscillator squeezing, we write the asymptotic form as:

$$R(\tilde{r}) \xrightarrow{r \rightarrow \infty} [\tilde{r} (\cos \delta_{\ell^*} j_{\ell^*}(k\tilde{r}) - \sin \delta_{\ell^*} \eta_{\ell^*}(k\tilde{r}))] e^{-\frac{z^2}{2b_{ho}^2}}, \quad (27)$$

where  $z = r \cos \theta$  and  $b_{ho}$  is the harmonic oscillator length associated to the squeezing potential. According to our estimates [22], the connection between  $d$  and  $b_{ho}$  is given by:

$$b_{ho} = \sqrt{\frac{2(d-2)}{(d-1)(3-d)}}, \quad (28)$$

which is given in units of the range of the particle-particle interaction.

The idea now is to interpret the  $d$ -wave function as an ordinary wave function in three dimensions whose radial part depends on  $\tilde{r}$ , and whose angular part is an ordinary spherical harmonic depending on  $\tilde{\theta}$  and  $\tilde{\varphi} = \varphi$ . Remembering that in 3D, as discussed below Eq.(2), we must have that  $m = \ell_{2b}$  we can then write:

$$\frac{R(\tilde{r})}{\tilde{r}^{\frac{d-1}{2}}} Y_{\ell_{2b}\ell_{2b}}(\tilde{\theta}, \varphi) = \sum_{\ell m} \frac{u_{\ell}(r)}{r} Y_{\ell m}(\theta, \varphi), \quad (29)$$

such that we expand the wave function in terms of the spherical harmonics expressed as function of the polar and azimuthal angles of the 3D relative coordinate.

From the equation above we can extract the projected radial wave functions as:

$$\frac{u_{\ell}(r)}{r} = \int d\Omega \frac{R(\tilde{r})}{\tilde{r}^{\frac{d-1}{2}}} Y_{\ell_{2b}\ell_{2b}}(\tilde{\theta}, \varphi) Y_{\ell m}^*(\theta, \varphi), \quad (30)$$

which, after integrating over  $\varphi$  (leading to  $\delta_{m,\ell_{2b}}$ ) and getting rid of the constants factors, becomes:

$$u_{\ell}(r) \propto r \int_0^{\pi} d\theta \sin \theta \frac{R(\tilde{r})}{\tilde{r}^{\frac{d-1}{2}}} P_{\ell_{2b}}^{(\ell_{2b})}(\cos \tilde{\theta}) P_{\ell}^{(\ell_{2b})}(\cos \theta) \quad (31)$$

whose asymptotic behavior can be computed by introducing Eq.(27). For a given  $r$ , the integrand in the equation above is just a function of  $\theta$  through Eqs.(24) and (25).

By fitting the  $u_{\ell}$  functions to the expected asymptotic behavior,

$$u_{\ell}(r) \xrightarrow{r \rightarrow \infty} r (\cos \delta_{\ell} j_{\ell}(kr) - \sin \delta_{\ell} \eta_{\ell}(kr)) \quad (32)$$

we can extract the phase shift for each partial wave  $\ell$ .

However, it is important to keep in mind that Eq.(32) gives the asymptotic behavior of the continuum wave functions in the ordinary, non-squeezed, 3D space. The effect of the confining external potential is not present in Eq.(32). In fact, in the case of no interaction between the particles, the  $d$ -phase shift,  $\delta_{\ell^*}$ , obtained from the asymptotic behavior (18) is trivially equal to zero, and the radial wave function is simply given by  $x j_{\ell^*}(kx)$ . When introducing this function into Eq.(31), and making use of Eq.(32), we can easily observe that the corresponding computed 3D phase shift is not zero. This non-zero phase shift, which we denote as  $\delta_{\text{free}}$ , reflects the effect of the confining external potential.

By definition, the phase shift is just the shift of the asymptotic wave function when compared to the free wave function. It is then clear that the phase shift in the confined 3D space,  $\delta_{\text{conf}}^{(\ell)}$ , is then given by:

$$\delta_{\text{conf}}^{(\ell)} = \delta_{\ell} - \delta_{\text{free}}, \quad (33)$$

where  $\delta_{\ell}$  and  $\delta_{\text{free}}$  are then the phase shifts obtained from Eqs.(31) and (32) for interacting and free particles, respectively.

We shall later show that  $\delta_{\text{conf}}^{(\ell)}$  is actually independent of  $\ell$ , which permits to associate a single phase shift  $\delta_{\text{conf}} \equiv \delta_{\text{conf}}^{(\ell)}$  to the two-body continuum state in the relative  $\ell_{2b}$ -wave in the squeezed 3D space. Furthermore, we shall also show the nice result that  $\delta_{\ell^*} = \delta_{\text{conf}}$ , which in fact means that the phase shifts obtained with the  $d$ -method are actually the phase shifts in the squeezed 3D space, and therefore they can be directly used to compute the cross section in the 3D space, which is given by the simple well-known formula:

$$\sigma = \frac{4\pi}{k^2} (2\ell_{2b} + 1) \sin^2 \delta_{\ell^*}. \quad (34)$$

### III. RESULTS

In this section we show the results for the key quantities analyzed in the previous section for two-body continuum states, i.e., critical dimension, scattering length, and phase-shifts. The derivations have been carried out assuming a square-well potential, and therefore the derived formulae, which of course depend on the dimension  $d$ , will depend as well on the square-well parameter,  $S_0$ . This dependence has been obtained in a very specific model, and provides results that, in principle, are not universal. However, as we shall show, it is possible to extract a universal behavior, such that the square-well results previously derived can be exported to any short-range potential.

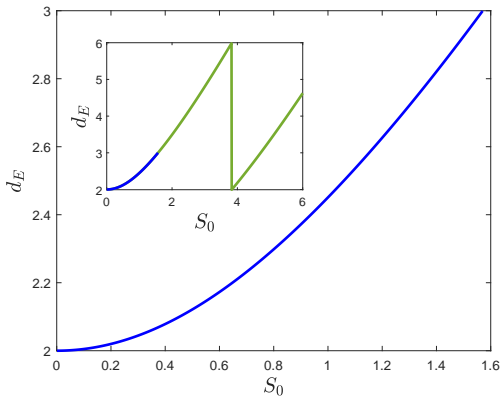


FIG. 1: The critical dimension,  $d_E$ , for  $s$ -waves, as a function of the potential parameter,  $S_0$ , defined in Eq.(10).

### A. Critical dimension

The critical dimension,  $d_E$ , is obtained by solving Eq.(12) as function of  $S_0$ . This dimension always exists for relative  $s$ -waves ( $\ell_{2b} = 0$ ), which is particularly relevant, since this is the dimension for which the Efimov effect arises in the three-body case.

The resulting dependence, shown in Fig. 1 for  $\ell_{2b} = 0$ , is a smoothly increasing function of  $S_0$ , changing from  $d_E = 2$  at  $S_0 = 0$ , to  $d_E = 3$  for  $S_0 = \pi/2$ . This reflects the fact that an infinitely small attractive potential is, for relative  $s$ -waves, sufficient to bind for  $d = 2$ , but a finite potential is necessary to support bound states as the dimension approaches  $d = 3$ . The value of  $S_0 = \pi/2$  for  $d = 3$  is the well-known critical size for binding in a square-well. Note also that, as shown in Eq.(13), for  $d = 3$  the values of the critical dimension,  $d_E$ , appear for the  $S_0$  values matching with the zeros of  $J_{-1/2}(S_0)$ , which are given by  $S_0 = (2n+1)\pi/2$ , with  $n = 0, 1, 2, \dots$ .

Increasing the attraction of the potential still smoothly increases  $d_E$  above 3, as shown in the inset of Fig. 1. This behavior is abruptly broken by a sudden downwards jump at  $S_0 = 3.83171$ , where a second bound state appears at zero energy. The following increase is the beginning of repeating this behavior reflecting the discrete increase of bound states. In fact, again, we can from Eq.(13) see that for  $d = 2$  the  $d_E$  values for which new bound states appear are determined by the zeros of  $J_{-1}(S_0) = -J_1(S_0)$ , whose first three values are  $S_0 = 3.83171, 7.01559, 10.17347$ , and which give the position of the jumps in the curve shown in the inset of Fig. 1.

The square-well parameter is by definition not a universal quantity that could be used for other short-range potentials. Instead, in order to pursue such a universality, we turn to the scattering length for  $d = 3$ , which is a unique characteristic for any short-range potential, as well as definable, measurable, and reflecting a gross property independent of potential details. It determines

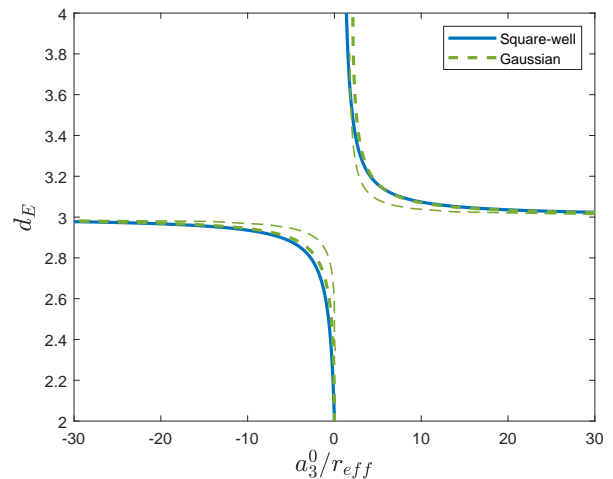


FIG. 2: The critical dimension,  $d_E$ , as a function of the scattering length,  $a_{d=3}^{(\ell_{2b}=0)}/r_{\text{eff}}$ , for the square-well (blue thick solid) and the Gaussian potentials (green thick dashed). The dimension  $d_E$  corresponds to the appearance of the first bound state. The green thin-dashed curve shows the  $d_E$ -values corresponding to the appearance of the second bound state with the Gaussian potential.

rather accurately all low-energy scattering properties, and as such is a universal quantity.

Although in principle possible as well for relative angular momenta larger than zero, universality features are specially relevant for  $s$ -waves, for which the wave function can more easily extend beyond the range of the interaction, becoming then less sensitive to the details of the potential. As shown in Eq.(22), for small energy the phase shifts behave as  $E^{(2\ell_{2b}+d-2)/2}$ , meaning that the  $s$ -wave scattering clearly dominates in the low-energy limit, and for this reason we shall focus here on universal behavior in the  $\ell_{2b} = 0$  case (an exception could be the case, not considered here, of two identical fermions, for which a relative  $s$ -wave is not possible [33]).

In Fig. 2 we show the critical dimension,  $d_E$ , as a function of  $a_{d=3}^{(\ell_{2b}=0)}$  for both square-well and Gaussian potentials. Different length units have been considered, and we have found that clearly the length scale with the effective range,  $r_{\text{eff}}$ , provides the most satisfactory universal behavior. This is in accordance with the findings for three-body systems [34]. The results for the two potentials are pretty close to each other, and we therefore have, to a very large extent, the desired, accurate universal function,  $d_E$ , as function of scattering length in units of the effective radius, both obtained in the ordinary three dimensions. This is what shown by the two thick curves in the figure, solid (blue) and dashed (green), which have been obtained with potential strengths such that  $d_E$  corresponds to the appearance of the first bound state, i.e., to potential strengths unable to bind the system in three dimensions.

In principle one could still increase  $S_0$  such that a sec-

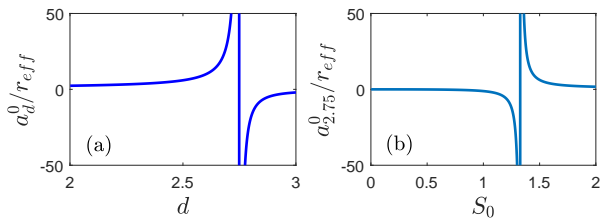


FIG. 3: (a) Scattering length,  $a_d^{(\ell_{2b}=0)}$ , as function of  $d$  for  $S_0 \simeq 4/3$ , such that  $d_E = 2.75$ . (b) Scattering length as function of  $S_0$  for  $d = 2.75$ .

ond bound state appears (as indicated by the jump in the curve shown in the inset of Fig. 1). As exemplified in previous works, the depth of the two-body potential could be an important factor for universality [34, 35]. Although this interesting relationship goes beyond the scope of this work, we show in Fig. 2, as an indication, the curve (thin-dashed) obtained for the critical dimension  $d_E$  corresponding to the appearance of the second bound state with the Gaussian potential. As we can see, this curve does not follow the universal curve obtained when  $d_E$  indicates the appearance of the first bound state.

The scattering length and effective range ratio for  $\ell_{2b} = 0$  and  $d = 3$  is therefore adopted as the easy accessible universal quantity. This has the advantage of requiring only one adjustment, the  $a_{d=3}^{(\ell_{2b}=0)}/r_{\text{eff}}$  ratio, when two potentials should be compared. Another possibility could perhaps be to use the same  $a_d^{(\ell^*)}$  for different potentials as defined in Eq.(16), or may be the same ratio between  $a_d^{(\ell^*)}$  and the corresponding  $d$ -dependent effective range. However, this would require calculation with different potentials for any  $d$ . The simplicity of the method would be lost, and we therefore we maintain the simple procedure.

### B. Scattering length

In any case, even if not used in the universal curve shown in Fig. 2, a given two-body potential, has associated a different scattering length for different values of the dimension  $d$ , as shown in Eq.(16) for the case of the square-well potential.

This  $d$ -dependent scattering length is a function of  $S_0$ , as shown in Fig. 3 for the square-well potential and  $\ell_{2b} = 0$ . The left and right parts show the dependence on  $d$  for a given  $S_0$  ( $S_0 \simeq 4/3$  such that  $d_E = 2.75$ ), and on  $S_0$  for a given  $d$  ( $d = 2.75$ ), respectively. If desired  $S_0$  can, through Fig. 1, be substituted by  $a_{d=3}^{(\ell_{2b}=0)}$ . The qualitative features are precisely the same.

The most pronounced feature is that the scattering length diverges at the critical dimension,  $d_E$ , see Fig. 3a. For  $S_0 \simeq 4/3$  we can see from Fig. 1 that  $d_E \approx 2.75$ , which is the  $d$ -value where the divergence of the scattering length shows up. This demonstrates the existence of a zero-energy bound state for this dimension. The picture

would be very similar for other values of  $S_0$ , where the zero-energy would appear at another  $d$ . For illustration, we show in Fig. 3b the other dependence of the scattering length as a function of  $S_0$  for given  $d$  ( $d = 2.75$ ). Again we observe a divergence of  $a_d^{(\ell_{2b}=0)}$  for a specific  $S_0$ ,  $S_0 \approx 4/3$ , which agrees with the value observed in Fig. 1 for  $d_E = 2.75$ , and defines the parameter set producing a zero-energy bound state.

### C. Phase-shifts

The phase-shifts contain the crucial information about the continuum states. They provide the information about the asymptotic behavior of the wave function, and they are the key ingredient to obtain an important observable like the cross sections.

In Fig. 4 we show the dependence of the  $s$ -wave phase shifts on the dimension  $d$  and on the energy (through  $\kappa$ , Eq.(6)). Each sub-figure compares four computed phase-shifts as function of the  $d$  for given values of  $\kappa/S_0$ .

The first two curves on each panel, thick-solid-black and thick-dashed-red, are the analytic square-well results in Eq.(20) and the related low-energy approximation in Eq.(22), respectively. Not surprisingly, we find the approximation improves with decreasing energy (decreasing  $\kappa$ ), but apparently also with increasing  $d$ . The mathematical reason can be found in the size of the  $d$ -dependent expansion parameter leading to Eq.(22). The parameters for the square-well potential have been chosen such that  $d_E = 2.50$ . The consequence is that for this value of  $d$ , as mentioned below Eq.(21), the low energy curves (thick-dashed-red) always take the value  $\delta_{\ell^*} = \pi/2$ .

For  $d = 2$  the low-energy phase-shifts are always  $\pi$  corresponding to a bound state. The exact model results are also close to  $\pi$  for  $d \approx 2$  and sufficiently small energies. The validity range of the low-energy expansion seem to be energies less than  $\kappa/S_0 \lesssim 0.001$ . For all these lower energies we observe a very sharp transition around  $d_E$  from phase-shifts of  $\pi$  to zero moving towards larger  $d$ -values. This behavior is connected to the general property of at least one bound state for any attraction for  $d = 2$  and in our case for  $d < d_E$ . The phase shift is passing  $\pi/2$  and a bound state of zero energy appears for  $d = d_E$ . For  $d > d_E$  there is no bound state, but a negative centrifugal barrier leading to phase-shifts close to zero, whereas there is at least one bound state for  $d < d_E$ , perhaps also conditions corresponding to a resonance with phase shifts  $\pi$ .

In Fig. 4 the results arising from the use of a Gaussian potential are also shown. To investigate the proper comparison between different potentials we first consider the square-well and the Gaussian potentials having the same scattering length ratio to the interaction range,  $r_0$ , for  $d = 3$ . The results for the Gaussian case are given by the thin-solid-blue curves. When compared to the square-well results (thick-solid-black) we see that both curves are quantitatively very similar, although the agreement

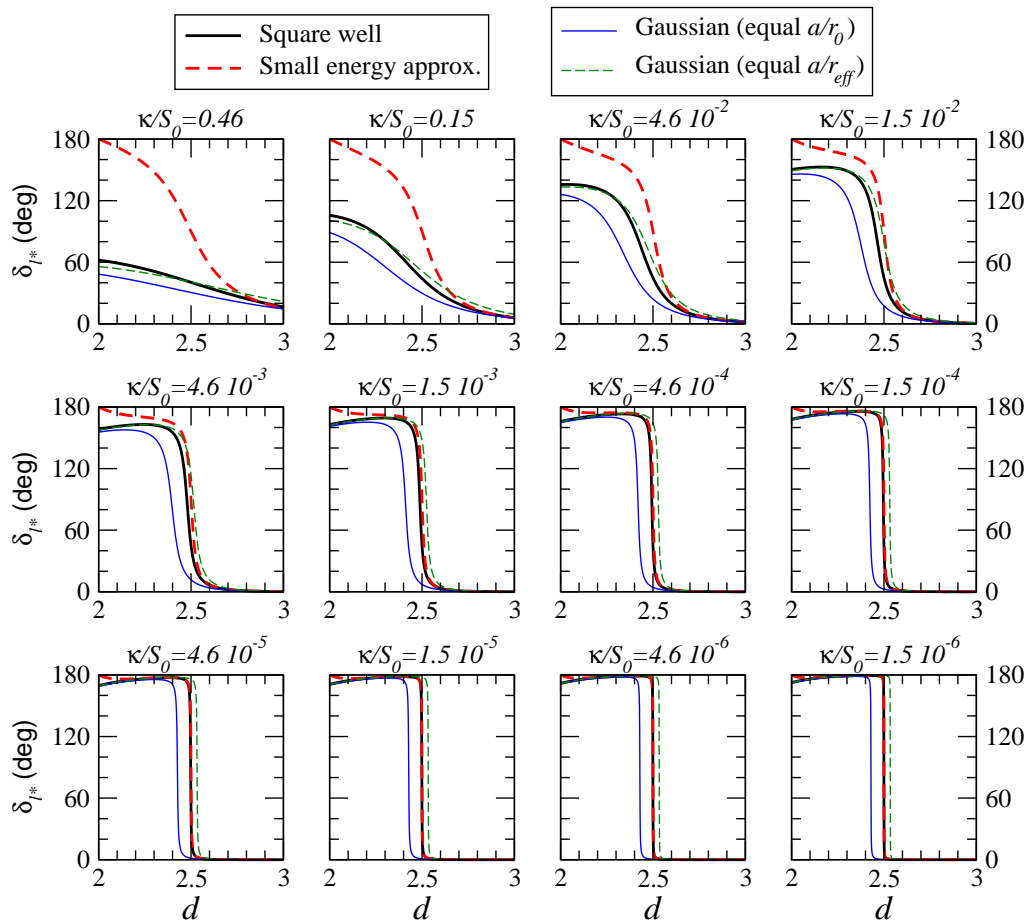


FIG. 4: Phase shifts,  $\delta_{\ell^*}$ , for  $\ell_{2b} = 0$  as function of  $d$  for different values of  $\kappa/S_0$ . The thick-solid-black curves are square-well results from Eq.(22), the thick-dashed-red curves are the square-well low-energy approximation from Eq.(21), the thin-solid-blue curves are for a Gaussian interaction comparing results for equal  $a_{d=3}^{(\ell_{2b}=0)}/r_0$  (scattering length divided by the Gaussian or square-well range) in 3D, and the thin-dashed-green curves are for a Gaussian interaction comparing results for equal  $a_{d=3}^{(\ell_{2b}=0)}/r_{\text{eff}}$  (scattering length divided by effective range) in 3D. The potential parameters produce  $d_E = 2.50$  for the square-well interaction.

between them is not perfect. In fact, the Gaussian potential constructed as mentioned above leads to a critical dimension  $d_E = 2.43$ , which implies that the crossing through  $\delta_{\ell^*} = \pi/2$  at low energies can be easily distinguished from the one of the square-well potentials, which happens at  $d_E = 2.50$ .

However, when the Gaussian potential is constructed having the same ratio between the scattering length and the effective range as in the square-well potential for  $d = 3$ , we then observe a clearly better agreement between both cases, as seen when comparing the thin-dashed-green and the thick-solid-black curves in Fig. 4 (the Gaussian potential has now  $d_E = 2.53$ ). The universal function describing the critical dimension as function of the scattering length divided by the effective range is therefore also valid for continuum states. This result is consistent with the universal curve shown in Fig. 2, also a function of  $a_{d=3}^{(\ell_{2b}=0)}/r_{\text{eff}}$ .

This is very reassuring, because we can then compare potentials with the same gross properties like scatter-

ing length and effective range, and claim the computed universal relation between phase shifts and dimension. In other words one can use the analytic square-well results and translate to any other potential by use of the potential-independent parameters, scattering length and effective range.

#### D. Cross sections

As described in Section II F, the  $d$ -dimensional wave function is interpreted as a wave function in the squeezed 3D space. As shown in Eq.(29), this wave function can be expanded in terms of the usual spherical harmonics, which permits to extract the projected radial wave functions  $u_\ell(r)$  as shown in Eq.(31).

In Fig. 5 we show, for  $\ell_{2b} = 0$ , the large distance part of the  $u_\ell(r)$  functions after the calculation in Eq.(31) for  $d = 2.9$ ,  $\ell = 0$  (black), 10 (red), and 40 (blue), and three different energies,  $E = 1$  (a),  $E = 0.1$  (b), and  $E = 0.01$



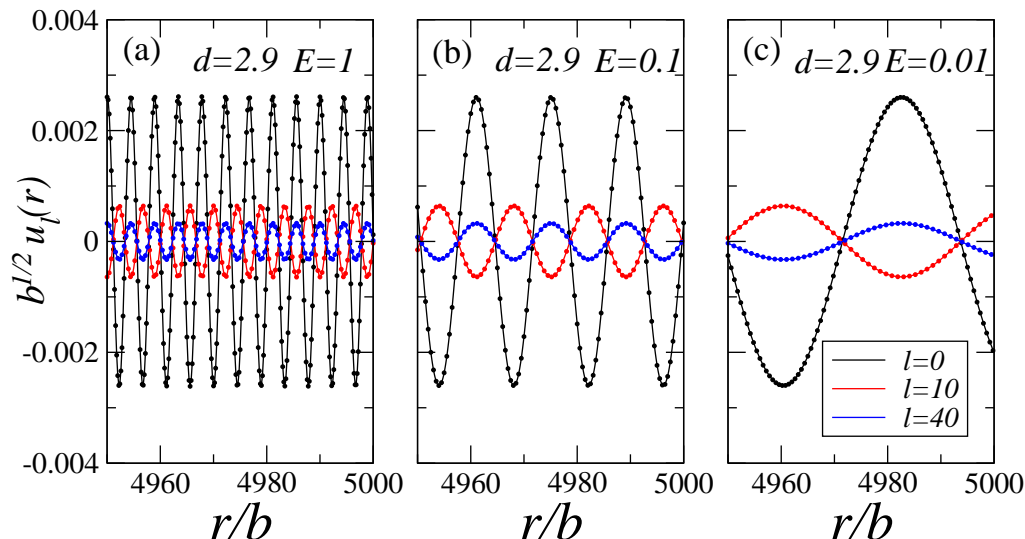


FIG. 5: Projected radial wave functions  $u_\ell(r)$  for  $\ell_{2b} = 0$ ,  $d = 2.9$ , and  $\ell = 0$  (black), 10 (red), and 40 (blue) and the Gaussian potential in Ref. [24]. The incident energy (in units of  $\hbar^2/(\mu b^2)$ ) is equal to 1 (a), 0.1 (b), and 0.01 (c). The solid curves are the results from Eq.(31), and the dots are the asymptotic behavior given in Eq.(32). The wave functions,  $u_\ell(r)$ , and the radial coordinate,  $r$ , are multiplied by  $b^{1/2}$  and divided by  $b$ , respectively, to make them dimensionless ( $b$  is the range of the potential).

(c) in units of  $\hbar^2/(\mu b^2)$ , where  $b$  is the range of the Gaussian two-body interaction used in the calculation. To be precise, we have used the Gaussian two-body potential given in Ref. [24], for which  $d_E = 2.75$ . In the figure we have multiplied  $u_\ell(r)$  by  $b^{1/2}$  and divided  $r$  by  $b$  in order to make both quantities dimensionless.

We can see that the larger  $\ell$ , the smaller the weight of the corresponding  $u_\ell(r)$  wave function. Therefore, one would expect that for sufficiently high values of  $\ell$ , the contribution of the  $u_\ell$  wave functions to the total wave function (29) can be neglected. In general, the larger the squeezing, the larger the number of  $\ell$ -values contributing. In fact, for  $d = 3$  only the  $u_{\ell=0}(r)$  function enters.

After matching the  $u_\ell$  functions with the analytic asymptotic behavior in Eq.(32) we can extract the  $\delta_\ell$  phase shifts. The result of this matching is shown in the figure by the dots, which we can see lie very much on top of the solid curves. We can also see that, as expected, the smaller the energy, the slower the oscillations of the wave functions. An important point in the figure is that, for each energy  $E$ , all the wave functions, independently of  $\ell$ , have the zeros at the same  $r$ -values. Although not shown in the figure, this happens no matter the value chosen for the dimension  $d$ . Therefore, as one could expect, it is possible to assign a single phase shift,  $\ell$ -independent, to the 3D wave function introduced in Eq.(29).

We illustrate this same result in Fig. 6, where we show  $\sin^2 \delta_\ell$  as a function of  $\ell$  for the case in Fig. 5a, i.e.,  $\ell_{2b} = 0$ ,  $d = 2.9$ , and  $E = 1$ . The different curves in the figure correspond to different values of the radial coordinate  $r$  used to match the computed  $u_\ell(r)$  function and the asymptotic behavior in Eq.(32). The result is that the larger the value of  $r$  chosen for the matching, the closer the curve to a horizontal line, corresponding to a constant

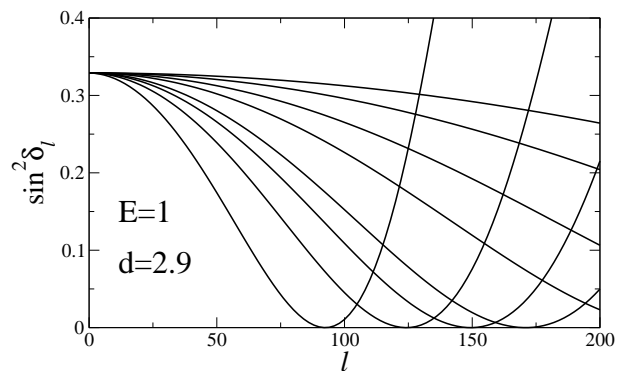


FIG. 6: Value of  $\sin^2 \delta_\ell$ , as a function of the angular momentum  $\ell$ , for the  $E = 1$  case in Fig. 5. The different curves correspond to different values of the large  $r$ -values used to extract  $\delta_\ell$ . The larger the  $r$ -values, the closer the curve to a constant value of  $\delta_\ell$ .

value of  $\delta_\ell$ . This is due to the fact that the larger the value of  $\ell$ , the farther one has to go in the wave function in order to get the correct asymptotic behavior. Again, the results shown in Fig. 6 are qualitatively the same as the ones obtained for a different value of  $d$  and a different energy.

Finally, as mentioned in Eq.(33), the phase shift,  $\delta_{\text{conf}}$ , in the squeezed 3D space is not given just by  $\delta_\ell$ , but by the shift of the wave function for two interacting particles compared to the wave function corresponding to two free particles. The phase shift obtained from Eq.(32) for two non-interacting particles is what in Eq.(33) is denoted by  $\delta_{\text{free}}$ .

In Fig. 7 we show  $\delta_\ell$ ,  $\delta_{\text{free}}$ ,  $\delta_{\text{conf}}$ , and  $\delta_{\ell^*}$  as a function

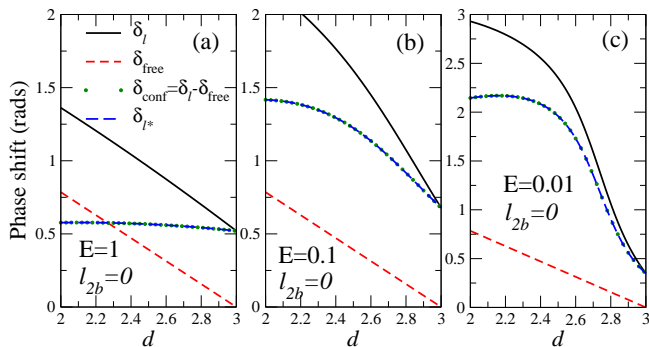


FIG. 7: For  $\ell_{2b} = 0$ , values, as a function of  $d$ , for the phase shifts  $\delta_\ell$  (solid-black),  $\delta_{\text{free}}$  (dashed-red),  $\delta_{\text{conf}} = \delta_\ell - \delta_{\text{free}}$  (dot-green), and  $\delta_{\ell^*}$  (long-dashed-blue), for the same potential and energies as in Fig. 5.

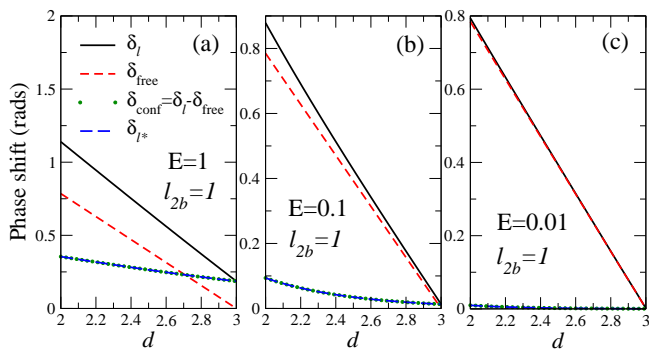


FIG. 8: The same as Fig.7 for  $\ell_{2b} = 1$ .

of  $d$  for the same Gaussian potential as in Fig. 5, and the same three energies. The phase shifts are given by the solid-black, dashed-red, dot-green, and long-dashed-blue curves, respectively.

Except for  $d = 3$ , where by definition they are the same, we can see that  $\delta_\ell$  and the phase shift computed directly with the  $d$ -method,  $\delta_{\ell^*}$ , are very different. Also, when the two particles do not interact, the phase shift,  $\delta_{\text{free}}$ , obtained from Eq.(32) is clearly different from zero (except of course for  $d = 3$ , where the asymptotics in Eq.(32) is exact). The important result is that, as shown by the dotted curves in the figure, the difference between  $\delta_\ell$  and  $\delta_{\text{free}}$ , that is,  $\delta_{\text{conf}}$ , coincides perfectly with  $\delta_{\ell^*}$ , i.e., with the phase shift obtained directly from the  $d$ -method.

Therefore, as anticipated in Section IIF, the phase shifts obtained with the  $d$ -method are the phase shifts in the squeezed 3D space, and they can be used to compute the cross section in the 3D space.

The result shown in Fig. 7 is actually general, not restricted to the  $\ell_{2b} = 0$  case. As an illustration we show in Fig. 8 the same as in Fig. 7 but for  $\ell_{2b} = 1$ . As we can see, the equality  $\delta_{\text{conf}} = \delta_{\ell^*}$  is also perfectly obtained, even in the case of very small energy, Fig. 8c, where  $\delta_\ell$  and  $\delta_{\text{free}}$ , are very similar, leading to very small values of the true phase shift.

#### IV. SUMMARY AND CONCLUSIONS

In this work we have used the  $d$ -method in order to investigate two-body continuum states in a squeezed scenario. The method describes the system in a non-integer dimensional space, which can be later translated to the usual 3D space with an external confining potential. The  $d$ -method is technically simpler, since the degrees of freedom associated to the external field do not enter in the formalism.

We focus on two-body properties for short-range potentials in non-integer geometry by use of a square-well potential. The details are independent of this practical choice of the potential.

We first derive conditions for bound states expressed by the square-well parameter. The depth-radius combination has to be large enough to support at least one bound state. We show how the threshold value of the dimension for binding is uniquely determined by the square-well parameter. This is in close analogy to three dimensions, but for smaller dimensions less attraction is necessary, and for  $d = 2$  even infinitesimally small attraction provides binding.

The point of zero energy binding defines the Efimov dimension,  $d_E$ , since for this dimension the Efimov effect may become effective by adding another particle. We have derived the equation determining the value of  $d_E$  as a function of the strength of the square-well potential. This value of  $d_E$  is shown to correspond to infinite scattering length, which in turn has also been derived as a function of the same strength for each dimension  $d$ .

We have closed the theoretical part of this paper deriving the expressions for the  $d$ -dependent phase shifts as a function of the potential strength. These phase shifts have also been related to the ones corresponding to the physical squeezed 3D space.

The main purpose of the illustrations shown in this work is to show that, even if the derived expressions, obtained for a square-well two-body interaction, are not necessarily universal, it is however possible, using the proper length and energy units, to obtain a universal behavior, independent of the details of the potential, for the Efimov dimension  $d_E$  as well as for the phase shifts.

In particular, focusing on the dominant  $s$ -wave case, we have shown that the critical dimension  $d_E$  follows a universal path when plotted as a function of  $a_{d=3}^{(\ell=0)}/r_{\text{eff}}$ , showing that the effective range in three dimensions is the appropriate length unit. Given the value of  $a_{d=3}^{(\ell=0)}/r_{\text{eff}}$  for any two-body short-range potential it is then possible, by means of the universal curve, to obtain the corresponding dimension  $d_E$ .

It is reassuring that potentials having the same value of the  $a_{d=3}^{(\ell=0)}/r_{\text{eff}}$  ratio follow as well a pretty much universal curve for the phase shifts as a function of the dimension and for given values of  $\kappa/S_0$ . In other words, for the universal curve to show up, the incident momentum has to be taken in units of  $S_0$ , which contains the dependence

on the strength of the potential.

Finally, we have related the computed phase shifts in the  $d$ -method with the ones corresponding to a squeezed 3D space. This is done by considering the  $d$ -dimensional two-body wave function as an ordinary wave function in 3D, but squeezing the coordinate along the direction of the external field after inclusion of a scale parameter. When this is done, we have shown that, in case of non-interacting particles, the usual asymptotic form of the continuum wave functions in three dimensions gives rise to non-zero phase shifts,  $\delta_{\text{free}}$ . This is simply reflecting the presence of the squeezing potential. When the interaction is introduced, the relevant phase shift is the difference between the new computed phase shift and  $\delta_{\text{free}}$ . We have shown that this difference,  $\delta_{\text{conf}}$ , is precisely the same as the phase shift obtained directly from the  $d$ -method. This result opens the door to using the  $d$ -computed phase shifts directly in order to obtain the cross sections in a squeezed scenario.

In conclusion, we have investigated and illustrated two-body scattering processes in an analytic schematic model. The cross section behavior and the insight obtained are very hard to imagine found in any other way. Such results are, to a large extent, universal, that is independent of the details of the employed short-range potentials. The translation from  $d$  to external field is necessary, available and at least a semi-accurate description. The perspective in our investigations is that scattering between particles confined by deformed external fields may be useful tools in investigations of for example structures related to Efimov physics. Transitions between other dimensions may

also be of interest.

## Acknowledgments

This work has been partially supported by the Spanish Ministry of Science, Innovation and University MCIU/AEI/FEDER,UE (Spain) under Contract No. PGC2018-093636-B-I00.

## Appendix A: Bessel function properties

The two regular spherical Bessel functions with indices 0 and 1 are

$$j_0(z) = \frac{\sin z}{z}, \quad j_1(z) = \frac{\sin z}{z} - \frac{\cos z}{z^2}. \quad (\text{A1})$$

We have two useful identities between any,  $B_l$ , of the regular,  $j_l$ , and irregular,  $\eta_l$ , Bessel and Hankel,  $h_l^{(\pm)} = \eta_l \pm ij_l$  functions, that is

$$z \frac{dB_l(z)}{dz} = lB_l(z) - zB_{l+1}(z), \quad (\text{A2})$$

$$(2l+1)B_l(z) = z(B_{l+1}(z) + B_{l-1}(z)). \quad (\text{A3})$$

Limits for zero arguments are useful. For  $z \rightarrow 0$  we have

$$j_l(z) \rightarrow \frac{z^l}{(2l+1)!!}, \quad \eta_l(z) \rightarrow \frac{(2l+1)!!}{(2l+1)} \frac{1}{z^{l+1}}. \quad (\text{A4})$$

- 
- [1] T. K ohler, K. G oral, and P. S. Julienne, *Rev. Mod. Phys.* 78, 1311 (2006).
- [2] I. Bloch, J. Dalibard, and W. Zwerger, *Rev. Mod. Phys.* 80, 885 (2008).
- [3] C. Chin, R. Grimm, P. Julienne, and E. Tiesinga, *Rev. Mod. Phys.* 82, 1225 (2010).
- [4] S. Deng, Z.-Y. Shi, P. Diao, Q. Yu, H. Zhai, R. Qi, and H. Wu, *Science* 353, 371 (2016).
- [5] D. Hove, E. Garrido, P. Sarriguren, D. V. Fedorov, H. O. U. Fynbo, A. S. Jensen, N. T. Zinner, *J. Phys. G: Nucl. Part. Phys.* 45, 073001 (2018).
- [6] V. M. Efimov, *Phys. Lett. B* 33, 563 (1970).
- [7] B. Simon, *Ann. Phys.* 97, 279 (1976).
- [8] L.D. Landau, E.M. Lifshitz, *Quantum Mechanics: Non-Relativistic Theory*, Pergamon Press Ltd., 1977, p. 163.
- [9] E. Nielsen, D.V. Fedorov, A.S. Jensen, and E. Garrido, *Phys. Rep.* 347, 373 (2001).
- [10] A.S. Jensen, K. Riisager, D.V. Fedorov, and E. Garrido, *Rev. Mod. Phys.* 76, 215 (2004).
- [11] T. Frederico, A. Delfino, L. Tomio, M.T. Yamashita, *Prog. Part. Nucl. Phys.* 67, 939 (2012).
- [12] N T Zinner and A S Jensen *J. Phys. G: Nucl. Part. Phys.* 40, 053101 (2013).
- [13] P. Naidon, S. Endo, *Rep. Prog. Phys.* 80, 056001 (2017).
- [14] E. Garrido, *Few-body Syst.* 59, 17 (2018).
- [15] J. Levins, P. Massignan, and M.M. Parish, *Phys. Rev. X* 4, 031020 (2014).
- [16] M.T. Yamashita, F.F. Bellotti, T. Frederico, D.V. Fedorov, A.S. Jensen, N. T. Zinner, *J. Phys. B: At. Mol. Opt. Phys.* 48, 025302 (2015).
- [17] J.H. Sandoval, F.F. Bellotti, A.S. Jensen, and M.T. Yamashita, *J. Phys. B: At. Mol. Opt. Phys.* 51, 065004 (2018).
- [18] D.S. Rosa, T. Frederico, G. Krein, and M.T. Yamashita, *Phys. Rev. A* 97, 050701(R) (2018).
- [19] E. R. Christensen, A.S. Jensen, and E. Garrido, *Few-body Syst.* 59, 136 (2018).
- [20] E. Garrido, A.S. Jensen, and R.  lvarez-Rodr guez, *Phys. Lett. A* 383, 2021 (2019).
- [21] E. Garrido and A.S. Jensen, *Phys. Rev. Research* 1, 023009 (2019).
- [22] E. Garrido and A.S. Jensen, *Phys. Rev. Research* 2, 033261 (2020).
- [23] A. Messiah, *Quantum Mechanics Vol. I* pp 385, North-Holland Publishing Company Amsterdam
- [24] E. Garrido and A.S. Jensen, *Phys. Lett. A* 385, 126982 (2021).
- [25] L.W. Bruch and J.A. Tjon, *Phys. Rev. A* 19, 425 (1979).
- [26] T.K. Lim and B. Shimer, *Z. Phys. A* 297, 185 (1980).
- [27] E. Nielsen, D.V. Fedorov, and A.S. Jensen, *Phys. Rev. A* 56, 3287 (1997).
- [28] A. G. Volosniev, D.V. Fedorov, A.S. Jensen, N.T. Zinner,

- Eur. Phys. J. D 67, 95 (2013).
- [29] J.M. Vogels, C.C. Tsai, R.S. Freeland, S.J.J.M.F. Kokkelmans, B.J. Verhaar and D.J. Heinzen, Phys. Rev. A 56, R1067 (1997).
- [30] Ph. Courteille, R.S. Freeland, D.J. Heinzen, F.A. van Abeelen and B.J. Verhaar, Phys. Rev. Lett. 81, 69 (1998).
- [31] E. Nielsen, D. V. Fedorov, A. S. Jensen, Phys. Rev. Lett. 82, 2844 (1999).
- [32] M. A. Shalchi, M. T. Yamashita, M. R. Hadizadeh, E. Garrido, Lauro Tomio, T. Frederico, Phys. Rev. A 97, 012701 (2018).
- [33] E. Braaten and H.-W. Hammer, Phys. Rep. 428, 259 (2006).
- [34] P. Naidon, S. Endo and M. Ueda, Phys. Rev. Lett. 112, 105301 (2014).
- [35] P. M. A. Mestrom, T. Secker, R. M. Kroeze, and S. J. J. M. F. Kokkelmans, Phys. Rev. A 99, 012702 (2019).
- [36] C. G. Bollini, J. J. Giambiagi, Nuovo Cim 26, 619-621 (1962).